Molecular Dynamics

International Edition: DOI: 10.1002/anie.201509622
German Edition: DOI: 10.1002/ange.201509622

How Photoisomerization Drives Peptide Folding and Unfolding: Insights from QM/MM and MM Dynamics Simulations

Shu-Hua Xia, Ganglong Cui, Wei-Hai Fang, and Walter Thiel**

Abstract: *Photoswitchable azobenzene cross-linkers can control the folding and unfolding of peptides by photoisomerization and can thus regulate peptide affinities and enzyme activities. Using quantum mechanics/molecular mechanics (QM/MM) methods and classical MM force fields, we report the first molecular dynamics simulations of the photoinduced folding and unfolding processes in the azobenzene cross-linked FK-11 peptide. We find that the interactions between the peptide and the azobenzene cross-linker are crucial for controlling the evolution of the secondary structure of the peptide and responsible for accelerating the folding and unfolding events. They also modify the photoisomerization mechanism of the azobenzene cross-linker compared with the situation in vacuo or in solution.*

An efficient light-sensitive peptide can be constructed by cross-linking a photoswitchable small cross-linker molecule to the peptide backbone; photoinduced structural changes of the cross-linker can trigger reversible changes in peptide conformations. This kind of photoresponse can provide an avenue for probing and manipulating complex living systems.[1] The photoinduced conformational dynamics of peptides with built-in azobenzenes has been exploited to probe functional changes of proteins, to manipulate enzyme activities, and to control cell signaling.[2] However, a detailed mechanistic understanding of these processes at the atomistic level is still lacking.

Experimentally, time-resolved infrared spectroscopy was employed to monitor the conformational dynamics of cross-linked peptides; it was found that both folding and unfolding processes show complex spectral kinetics and strongly depend on the photoexcitation wavelength and on temperature.[3] Computationally, azobenzene-linked peptides were explored by classical molecular dynamics (MD) simulations.[4] However, in these studies, the initial nonadiabatic photoisomerization was not considered or was only simulated using a simple model potential, and the effects of the photoisomerization on the subsequent conformational dynamics of peptides were not investigated; moreover, only the photoinduced folding dynamics was simulated in those studies.[4] The unfolding dynamics of cross-linked peptides has rarely been explored experimentally because peptide unfolding processes are generally endothermic and difficult to study.[4f]

A salient dynamical feature of these cross-linked peptides is that their folding and unfolding processes are significantly accelerated compared with peptides without cross-linkers.[3a] This speedup must originate from the interaction between the cross-linker and the peptide. A thorough understanding of this interplay is crucial to rationalize the folding and unfolding dynamics of cross-linked peptides, to select appropriate cross-linkers, to optimize cross-linking positions, and eventually to control these photoinduced conformational changes. It is difficult to obtain detailed information on these interactions solely from experiment, and it is thus desirable to perform theoretical simulations, both for the initial photoisomerization and the subsequent folding and unfolding dynamics of azobenzene cross- linked peptides.

Numerous theoretical studies have explored the photoisomerization of azobenzene using static electronic structure computations and nonadiabatic dynamics simulations, but mostly only in vacuo or in solution.[5] Others have addressed photoswitching in azobenzene-linked biomolecules (RNA, DNA) and gold tips,[6,7] but to our knowledge, there are not yet any ab initio nonadiabatic dynamics simulations for azobenzene cross-linked with a peptide. In such a system, the external strain by the peptide is expected to influence the photoisomerization dynamics. Moreover, the strength of this strain can likely be adjusted by the secondary structure of the peptide (see Figure 1). To address these issues computationally, we have chosen the experimentally well-studied azobenzene cross-linked FK-11 peptide as our target system; this small 18-residue peptide has relatively short folding and unfolding timescales, and the azobenzene cross-linker exhibits high isomerization efficiency and large conformational changes.[3–5] To simulate the initial photoisomerization and the subsequent folding and unfolding dynamics of FK-11, we adopt a combined QM/MM and MM MD protocol, in which the photoisomerization is simulated using ab initio QM/MM nonadiabatic dynamics, while folding and unfolding processes are modeled using classical MD (see the Supporting Information for a detailed description).

We adopt the following notation to designate the four main conformations of the azobenzene cross-linker and the FK-11 peptide: *trans*-helix, *trans*-coil, *cis*-helix, and *cis*-coil; for example, *trans*-helix means that the azobenzene is in the *trans* form and the peptide is in the α-helix conformation. We first look at two typical trajectories illustrating the photoinduced folding and unfolding processes of FK-11. The top

[*] Dr. S.-H. Xia, Prof. Dr. G. Cui, Prof. Dr. W.-H. Fang
Key Laboratory of Theoretical and
Computational Photochemistry Ministry of Education
College of Chemistry, Beijing Normal University
Beijing 100875 (China)
E-mail: ganglong.cui@bnu.edu.cn
Prof. Dr. W. Thiel
Max-Planck-Institut für Kohlenforschung
Kaiser-Wilhelm-Platz 1, 45470 Mülheim an der Ruhr (Germany)
E-mail: thiel@mpg.kofo.de

Supporting information for this article is available on the WWW under http://dx.doi.org/10.1002/anie.201509622.

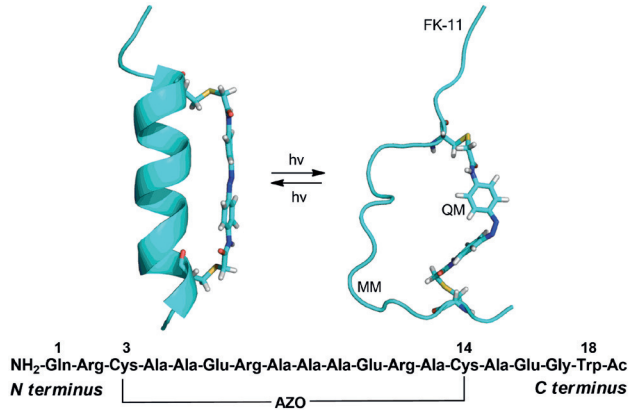

Figure 1. The FK-11 peptide in the α-helix (left) and random-coil (right) conformations. In the QM/MM computations, the QM region consists of the azobenzene cross-linker, while the MM region contains all other atoms (residues and water). Also shown is the sequence of the FK-11 peptide.

panel of Figure 2 shows consecutive snapshots of the photo-triggered folding dynamics from a typical trajectory starting from the *cis*-coil conformation. During the first picosecond,

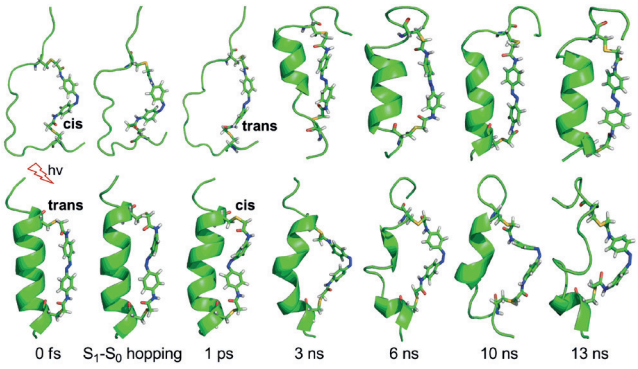

Figure 2. Consecutive snapshots of two typical folding and unfolding trajectories after *cis–trans* (top) and *trans–cis* (bottom) photoisomerization, respectively. The nonadiabatic dynamics simulations in the first picosecond were done at the QM/MM level, followed by classical MD dynamics (shown here up to 13 ns). The peptide chain runs downward from C to N terminus.

the S_1 state decays to the S_0 state generating *trans*-azobenzene; this *cis-trans* photoisomerization is so fast that the peptide remains in the coil conformation, because it is not able to respond on this time scale to the structural change of the azobenzene linker. The α-helix structure of the peptide starts to appear after about 3 ns; then, it gradually grows until 10 ns when a stable α-helix secondary structure is formed. In the final 3 ns of the simulation, there is no further obvious change in the secondary structure of the peptide. The bottom panel of Figure 2 shows snapshots of the photoinduced unfolding dynamics from a typical trajectory starting from the *trans*-helix conformation. After photoexcitation to the S_1 state, the azobenzene cross-linker isomerizes from the *trans* to *cis* form within 1 ps, without any obvious change in the overall α-helix structure of the peptide. After 3 ns, there is a visible stretching and bending in the α-helix structure with regard to the helical axis, but no unfolding yet. After 6 ns, the α-helix structure becomes partially unfolded. This process continues until the end of our simulation (13 ns) when most of the α-helix is unfolded, except for a small part close to the N terminus. Peptide unfolding is known to be thermodynamically unfavorable,[4f] and it is thus not surprising that during this process, we can still observe repeated re-folding events. By contrast, we do not see re-unfolding events in the folding trajectories. Evidently, the unfolding of the cross-linked peptide is slower and less facile than its folding (see the Supporting Information).

To explore the cross-linking effects on the folding and unfolding dynamics of FK-11, we have run two sets of 10 trajectories without the azobenzene cross-linker, starting from random-coil and α-helix conformations, respectively. In these runs we never see any folding and unfolding events within the 10 ns dynamics simulations, which clearly demonstrates that the azobenzene cross-linking does accelerate the folding and unfolding of the FK-11 peptide. Figure S4 shows snapshots from two representative trajectories, which illustrate that the α-helix and random-coil secondary structures do not change perceptibly during these simulations.[3]

The speedup of the folding and unfolding processes is caused by the external strain exerted by the cross-linker. This is reflected in the S···S distance between the two cysteine residues that are connected to the azobenzene cross-linker by two covalent C–S bonds. Taking the folding trajectory in the top part of Figure 3 as an example, the initial S···S distance of the peptide in the *cis*-coil conformation is about 15 Å, which happens to be somewhat larger than the axial length (ca. 13 Å) of *cis*-azobenzene (see panel (a) of Figure 3). Upon *cis–trans* photoisomerization of the cross-linker during the first picosecond, the peptide remains in the random-coil conformation, but the S···S distance in the FK-11 peptide increases within 1 ps to about 17 Å, close to the axial length of *trans*-

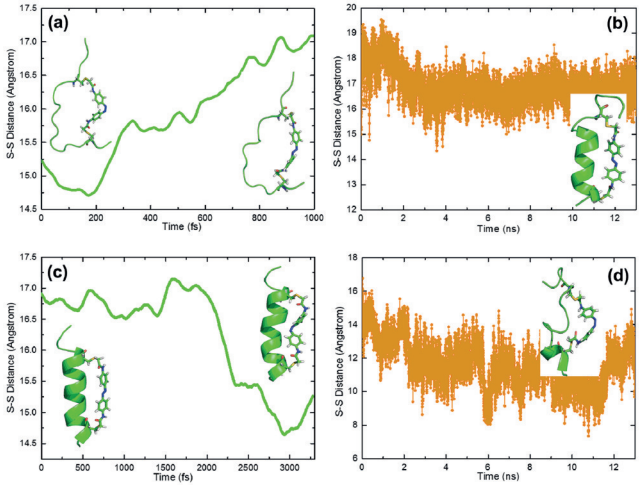

Figure 3. Time-dependent S···S distance in FK-11 during typical trajectories starting from the *cis*-coil (a,b) and *trans*-helix (c,d) conformations: a) initial nonadiabatic *cis–trans* photoisomerization, b) photo-induced folding dynamics, c) initial nonadiabatic *trans–cis* photoisomerization, and d) photoinduced unfolding dynamics.

azobenzene, followed by a further rise to ca. 19 Å in the first 2 ns. As discussed above, the peptide with the *trans*-azobenzene linker starts to evolve after 3 ns into the more stable α-helix structure to alleviate the excess strain introduced by the *cis–trans* photoisomerization; this is accompanied by a relaxation of the S···S distance, which then oscillates around the equilibrium value of about 17 Å in the α-helix (see panel (b) of Figure 3). In the unfolding trajectory, the initial S···S distance of the FK-11 peptide in the *trans*-helix conformation has the typical value of around 17 Å. After the ultrafast *trans–cis* photoisomerization of the linker, this distance rapidly decreases to about 15 Å within 1 ps (see panel (c) of Figure 3), which is still unfavorably high for the α-helix structure with *cis*-azobenzene linker. Hence the system further evolves towards the random-coil conformation, in which the S···S distance fluctuates considerably, with typical values of about 12 Å (see panel (d) of Figure 3).

The DSSP (dictionary of protein secondary structure) method[8] is an established tool to analyze the time-dependent evolution of secondary structures (coil, bend, turn, 3-helix, and α-helix). We have applied the DSSP analysis to two typical folding and unfolding trajectories of azobenzene cross-linked FK-11 (see Figure 4). Panel (a) shows the secondary-

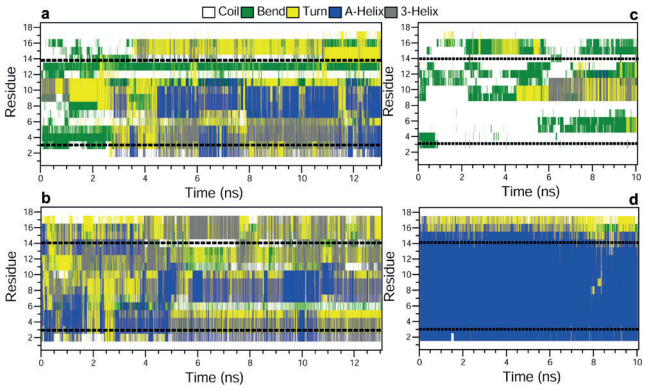

Figure 4. Time-dependent DSSP analysis for two typical folding and unfolding trajectories of azobenzene cross-linked FK-11 triggered by *cis–trans* (a) and *trans–cis* (b) photoisomerization, respectively. Also shown is the DSSP analysis for two trajectories of FK-11 without the azobenzene cross-linker starting from random-coil (c) and α-helix (d) conformations.

structure evolution for the photoinduced *cis–trans* folding trajectory starting from the *cis*-coil conformation. In the first 2 ns, the peptide is mainly composed of coil and bend secondary structure elements, except for residues 9–11, which alternatingly show turn and 3-helix motifs. Thereafter, the proportion of turn structures increases markedly until the first α-helix motifs arise among residues 7–10 after 2.8 ns, which are retained basically during the entire simulation (with very rare occurrences of turn and 3-helix features). The bend structure among residues 2–5 starts to evolve into turn and 3-helix structures after 2.5 ns and eventually into an α-helix structure after 3.5 ns. However, the latter is not as persistent as that among residues 7–10; it often interconverts with 3-helix and turn structures during the subsequent simulation. The turn structure among residues 14–16 appears after 4 ns and remains dominant thereafter, while the bend structure of residues 12–13 is preserved during the whole simulation.

Panel (b) shows the evolution for the photoinduced *trans–cis* unfolding trajectory starting from the *trans*-helix conformation. At the very beginning of the simulation, the α-helix structure is retained almost completely, except for a few turn and coil motifs. Among residues 12–16, it is converted to turn and 3-helix structures during the first 4 ns, and thereafter it is completely unfolded and never re-folded again. Among residues 6–10, there are repeated conversions between the α-helix and the turn and 3-helix structures, respectively, during the entire simulation. Among residues 1–5, the α-helix structure is unfolded after 5 ns, and re-folded again after 10 ns; hence, these unfolding and folding processes appear to occur less frequently than in the case of residues 6–10.

Panels (c) and (d) show the time-dependent DSSP results for two typical trajectories of the FK-11 peptide (without cross-linker) starting from random-coil and α-helix conformations, respectively. In the former, the predominant secondary structures of FK-11 are the coil, turn, and bend structures, which prevail in the whole 10 ns MD simulation; residues 1–3 always retain the coil structure, while α-helix structures are hardly formed, except occasionally among residues 4–6 and 8–12 [see panel (c)]. In the latter, the α-helix structure remains intact during the entire simulation for almost all FK−11 residues, except for residues 15–17 where the helix quickly unfolds and gives rise to dominant turn motifs [panel (d)].

These time-dependent DSSP features can be rationalized using the known α-helix propensities of residues.[8] Alanine has the highest α-helix propensity; hence, the more alanine residues the α-helix is composed of, the more likely will it be formed. In FK-11, residues 4–5, 8–10, 13, and 15 are alanine. It is thus not surprising that residues 6–10 are folded into an α-helix after 4 ns in the folding trajectory and remain so until the end of the simulation [panel (a)]. For residues 1–5, the folding trajectory shows fast formation of α-helix motifs, which however do not persist and frequently interconvert with 3-helix and turn motifs [panel (a)]; in this case, the influence of alanine residues 4–5 is counterbalanced by the low α-helix propensity of the cystein residue 3, which gives rise to repeated unfolding and re-folding events. Finally, the very low α-helix propensity of the glycine residue 17 may contribute to the strong preference for coil structures at the C terminus of FK-11 [residues 17–18, panel (a)]. The DSSP results for the unfolding trajectory [panel (b)] can be explained analogously.

The mutual interaction between the FK-11 peptide and the azobenzene cross-linker not only accelerates the folding and unfolding of FK-11 but also affects the photoisomerization mechanism of azobenzene. Table S1 collects $S_1 \rightarrow S_0$ hopping times and S_1–S_0 energy gaps at all hopping points, and specifies the final azobenzene conformation in all non-adiabatic dynamics trajectories. We find that 11 of 20 (55%) *cis*-coil trajectories evolve into the *trans*-isomer of azobenzene, while 6 of 14 (43%) *trans*-helix trajectories evolve into the *cis*-isomer. On the basis of these results, we estimate the *cis–trans* and *trans–cis* quantum yields to be 0.55 and 0.43;

given the small number of trajectories, these values are admittedly only crude estimates with large statistical uncertainties. Nevertheless, the *cis–trans* quantum yield is close to the results from previous gas-phase theoretical studies, for example, 0.58[5i] and 0.61–0.70;[5e] the *trans–cis* quantum yield is higher than the reported theoretical value of 0.17[5j] and the quoted experimental estimates of 0.20–0.25,[5j] but lies in the range of 0.30–0.46 reported by Toniolo et al.[5e] As a caveat, we emphasize again that our present ab initio QM/MM nonadiabatic dynamics simulations of azobenzene photoisomerization in the solvated FK-11 peptide simultaneously consider both environmental effects and the external strain exerted by the peptide, and are thus not directly comparable to previous theoretical studies in vacuo.[5]

The average $S_1 \rightarrow S_0$ hopping time (69 fs) in the trajectories starting from the *cis*-coil conformation is much shorter than that in the trajectories starting from the *trans*-helix conformation (621 fs). This trend is consistent with available experimental and theoretical studies in vacuo or in solution,[5] but the difference between the average hopping times is larger in the present case. Gas-phase electronic structure calculations indicate that the relevant S_1/S_0 minimum-energy conical intersection is closer to *cis*-azobenzene than to *trans*-azobenzene, which is an intrinsic factor favoring a faster *cis–trans* photoisomerization regardless of the actual environment, as found in previous work.[5] In the azobenzene cross-linked FK-11 peptide, there is an additional extrinsic factor, namely the external strain exerted by the peptide: the *trans*-helix conformation is clearly much stiffer than the *cis*-coil conformation. Hence, the *cis*-azobenzene moiety is more flexible in the random-coil conformation and can reach the relevant S_1/S_0 conical intersection more easily. By contrast, the *trans*-azobenzene linker in the α-helix conformation has to spend more time in attempts to approach the funnel region leading to the S_0 state.

The distribution of the $S_1 \rightarrow S_0$ hopping points is shown in Figure 5 with regard to three key dihedral angles: C2N3N4C5 (torsion around the central NN double bond), C1C2N3N4 and N3N4C5C6 (torsion of the two phenyl rings). As expected, the hops mostly occur at geometries with an almost perpendicular twist around the NN bond: the C2N3N4C5 dihedral angle is confined to a small range, around 100° and 90° for the *trans–cis* and *cis–trans* hops, respectively. With regard to the torsion of the phenyl rings, the hopping-point distribution is spatially localized (delocalized) for the *cis–trans* (*trans–cis*) photoisomerization. In the *cis–trans* case (red in Figure 5), the corresponding dihedral angles do not vary much: C1C2N3N4 between −20° and 20°; and N3N4C5C6 between −30° and 5°. These angles cover a much larger range in the *trans–cis* case (green in Figure 5): C1C2N3N4 between −73° and 52°; and N3N4C5C6 between −53° and 60°. In other words, with regard to the two phenyl torsions, the $S_1 \rightarrow S_0$ hopping region is spatially extended only in the case of the *trans–cis* photoisomerization.

Comparison of the distributions of these three key dihedral angles at the starting and hopping points confirms that the C2N3N4C5 dihedral angle is a key coordinate for describing the photoisomerization. It changes from about −170° to −100° in the *trans–cis* case and from about 10° to 80°

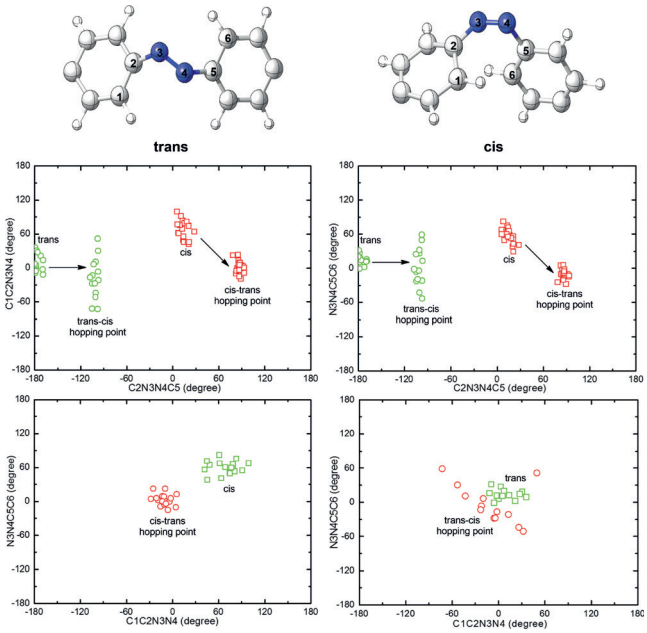

Figure 5. Distribution of important dihedral angles at the *trans–cis* (green) and *cis–trans* (red) $S_1 \rightarrow S_0$ hopping points in all nonadiabatic trajectories from the present work: with respect to C2N3N4C5 and C1C2N3N4 (middle left), C2N3N4C5 and N3N4C5C6 (middle right), C1C2N3N4 and N3N4C5C6 (bottom left), and C1C2N3N4 and N3N4C5C6 (bottom right).

in the *cis–trans* case (Figure 5). However, there are some differences with respect to the phenyl torsions. In the *trans–cis* case, the centroid of the distribution of the C1C2N3N4 and N3N4C5C6 dihedral angles does not shift notably when going from the starting to the hopping points (green), regardless of the appreciable spread of the distribution. By contrast, in the *cis–trans* case, the hopping point distribution remains clustered, but its centroid shifts significantly (red in Figure 5). The external strain exerted by the secondary structures of the FK-11 peptide is probably at least partly responsible for this different behavior. In the *cis–trans* photoisomerization, the peptide is in the random-coil conformation and thus very flexible; hence, the torsion of the two phenyl groups is facile and can easily follow the twist around the NN bond. Conversely, in the *trans–cis* case, the peptide is in the α-helix conformation and thus much stiffer; therefore, the torsion of the two phenyl groups is more difficult and falls behind the twist around the NN bond in most of the trajectories.

The photoisomerization modes observed in our present dynamics simulations differ to some extent from those reported for azobenzene in vacuo and solution. Previous nonadiabatic dynamics simulations have led to a consensus mechanism, in which the rotation of the azo group (a bicycle pedal-type motion) drives the photoisomerization.[5i,j] This process has been described as hula-twist motion of the nitrogen atoms,[5c] as purely rotational motion of the central CNNC moiety,[5l] and as rotation around the azo double bond, with minor involvement of nearby N−C bond rotations and NNC bending vibrations.[5h] These previous studies concluded that there is no large-amplitude phenyl torsion during photoisomerization (before the hop to the ground state).

We also observe the hula-twist motion of the nitrogen atoms in both the *trans–cis* and *cis–trans* photoisomerizations of the azobenzene cross-linker. However, we also see significant phenyl torsions around the C–N bonds in the *cis–trans* trajectories, which even appear to be concerted with the twist around the central azo bond, and there are changes of the C1C2N3N4 and N3N4C5C6 dihedral angles by more than 60° in the first 50 fs (see left panel of Figure S3 for a typical example). In comparison, the phenyl motions during *trans–cis* photoisomerization are relatively moderate in the initial stage (see right panel of Figure S3). These differences in the dynamics are caused by the different external strain exerted by the distinct secondary structures of the FK-11 peptide. As discussed above, the peptide in the α-helix conformation behaves like a spring and makes it much stiffer than in the random-coil conformation; hence, the torsions of the phenyl groups are frustrated in the *trans–cis* photoisomerization that starts from the α-helix conformation. By contrast, the peptide in the random-coil conformation behaves like a loose string, with little strain on the azobenzene cross-linker, so that large-amplitude torsions of the two phenyl groups can be observed in the *cis–trans* dynamics simulations that start from the random-coil conformation.

In summary, we have employed QM/MM and MM MD simulations to model the photoinduced folding and unfolding processes in a typical azobenzene cross-linked peptide (FK-11). We show that the cross-linking of a photoswitchable azobenzene can accelerate the folding and unfolding events in the FK-11 peptide. The interactions between the peptide and the azobenzene cross-linker play a key role in regulating the photoinduced evolution of the secondary structure of the peptide. These interactions also change the photoisomerization mechanism of the azobenzene cross-linker. The central CNNC rotation around the azo group remains the key motion during the *cis–trans* and *trans–cis* photoisomerizations, but the phenyl torsions play a different role in these two cases. Large-amplitude torsions of the phenyl rings are observed only in the *cis–trans* photoisomerization starting from the random-coil conformation, but not in the *trans–cis* case starting from the much stiffer α-helix conformation. The differences in peptide stiffness also cause much longer S_1 decay times for *trans–cis* photoisomerization (621 fs vs. 69 fs in the *cis–trans* case). The present study shows that the combined QM/MM and MM MD simulation protocol is useful for modeling photoinduced conformational changes of biomolecular systems.[9] We anticipate that this approach can also be applied to investigate photocontrol phenomena in other peptides, proteins, and biomaterials.

Acknowledgements

This work has been supported by the grants NSFC 21522302 (G.C.), NSFC 21520102005, and NSFC 21421003.

Keywords: azobenzene · conical intersections · folding and unfolding · nonadiabatic dynamics · quantum mechanics/molecular mechanics

How to cite: *Angew. Chem. Int. Ed.* **2016**, *55*, 2067–2072
Angew. Chem. **2016**, *128*, 2107–2112

[1] a) F. Zhang, O. Sadovski, S. Xin, G. Woolley, *J. Am. Chem. Soc.* **2007**, *129*, 14154–14155; b) S. Bhattacharya, H. Zhang, A. Debnath, D. Cowburn, *J. Biol. Chem.* **2008**, *283*, 16274–16278; c) L. Henchey, A. Jochim, P. Arora, *Curr. Opin. Chem. Biol.* **2008**, *12*, 692–697; d) R. Moellering, M. Cornejo, T. Davis, C. Del Bianco, J. Aster, S. Blacklow, A. Kung, D. Gilliland, G. Verdine, J. Bradner, *Nature* **2009**, *462*, 182–188; e) Y. Wu, D. Frey, O. Lungu, A. Jaehrig, I. Schlichting, B. Kuhlman, K. Hahn, *Nature* **2009**, *461*, 104–108; f) R. Airan, K. Thompson, L. Fenno, H. Bernstein, K. Deisseroth, *Nature* **2009**, *458*, 1025–1029; g) S. Samanta, G. Woolley, *ChemBioChem* **2011**, *12*, 1712–1723; h) N. Labòria, R. Wieneke, R. Tampé, *Angew. Chem. Int. Ed.* **2013**, *52*, 848–853; *Angew. Chem.* **2013**, *125*, 880–886; i) I. Tochitsky, A. Polosukhina, V. Degtyar, N. Gallerani, C. Smith, A. Friedman, R. Van Gelder, D. Trauner, D. Kaufer, R. Kramer, *Neuron* **2014**, *81*, 800–813; j) V. Gatterdam, R. Ramadass, T. Stoess, M. Fichte, J. Wachtveitl, A. Heckel, R. Tampé, *Angew. Chem. Int. Ed.* **2014**, *53*, 5680–5684; *Angew. Chem.* **2014**, *126*, 5787–5791.

[2] a) A. Beharry, G. Woolley, *Chem. Soc. Rev.* **2011**, *40*, 4422–4437; b) H. Dhammika Bandara, S. Burdette, *Chem. Soc. Rev.* **2012**, *41*, 1809–1825; c) M. Korbus, G. Balasubramanian, F. Müller-Plathe, H. Kolmar, F.-J. Meyer-Almes, *Biol. Chem.* **2014**, *395*, 401–412; d) B. Schierling, A.-J. Noël, W. Wende, L. Hien, E. Volkov, E. Kubareva, T. Oretskaya, M. Kokkinidis, A. Römpp, B. Spengler, A. Pingoud, *Proc. Natl. Acad. Sci. USA* **2010**, *107*, 1361–1366; e) P. Gorostiza, E. Isacoff, *Science* **2008**, *322*, 395–399; f) F. Zhang, K. Timm, K. Arndt, G. Woolley, *Angew. Chem. Int. Ed.* **2010**, *49*, 3943–3946; *Angew. Chem.* **2010**, *122*, 4035–4038; g) S. Samanta, C. Qin, A. Lough, G. Woolley, *Angew. Chem. Int. Ed.* **2012**, *51*, 6452–6455; *Angew. Chem.* **2012**, *124*, 6558–6561.

[3] a) E. Chen, J. Kumita, G. Woolley, D. Kliger, *J. Am. Chem. Soc.* **2003**, *125*, 12443–12449; b) G. Woolley, *Acc. Chem. Res.* **2005**, *38*, 486–493; c) J. Bredenbeck, J. Helbing, J. Kumita, G. Woolley, P. Hamm, *Proc. Natl. Acad. Sci. USA* **2005**, *102*, 2379–2384; d) J. Ihalainen, J. Bredenbeck, R. Pfister, J. Helbing, L. Chi, I. van Stokkum, G. Woolley, P. Hamm, *Proc. Natl. Acad. Sci. USA* **2007**, *104*, 5383–5388; e) J. Ihalainen, B. Paoli, S. Muff, E. Backus, J. Bredenbeck, G. Woolley, A. Caflisch, P. Hamm, *Proc. Natl. Acad. Sci. USA* **2008**, *105*, 9588–9593; f) F. Zhang, A. Zarrine-Afsar, M. Al-Abdul-Wahid, R. Prosser, A. Davidson, G. Woolley, *J. Am. Chem. Soc.* **2009**, *131*, 2283–2289.

[4] a) P. Nguyen, S. Park, G. Stock, *J. Chem. Phys.* **2006**, *124*, 025102; b) P. Nguyen, H. Staudt, J. Wachtveitl, G. Stock, *J. Phys. Chem. B* **2011**, *115*, 13084–13092; c) B. Paoli, M. Seeber, E. H. G. Backus, J. A. Ihalainen, P. Hamm, A. Caflisch, *J. Phys. Chem. B* **2009**, *113*, 4435–4442; d) B. Paoli, R. Pellarin, A. Caflisch, *J. Phys. Chem. B* **2010**, *114*, 2023–2202; e) T. Schrader, T. Cordes, W. Schreier, F. Koller, S.-L. Dong, L. Moroder, W. Zinth, *J. Phys. Chem. B* **2010**, *114*, 5219–5226; f) S. Englander, L. Mayne, *Proc. Natl. Acad. Sci. USA* **2014**, *111*, 15873–15880.

[5] a) S. Monti, G. Orlandi, P. Palmieri, *Chem. Phys.* **1982**, *71*, 87–99; b) T. Schultz, J. Quenneville, B. Levine, A. Toniolo, T. Martínez, S. Lochbrunner, M. Schmitt, J. Shaffer, M. Zgierski, A. Stolow, *J. Am. Chem. Soc.* **2003**, *125*, 8098–8099; c) M. Böckmann, N. Doltsinis, D. Marx, *J. Phys. Chem. A* **2009**, *113*, 745–754; d) C. Ciminelli, G. Granucci, M. Persico, *Chem. Eur. J.* **2004**, *10*, 2327–2341; e) A. Toniolo, C. Ciminelli, M. Persico, T. Martínez, *J. Chem. Phys.* **2005**, *123*, 234308; f) M. Böckmann, C. Peter, L. Site, N. Doltsinis, K. Kremer, D. Marx, *J. Chem. Theory Comput.* **2007**, *3*, 1789–1802; g) I. Conti, M. Garavelli, G. Orlandi, *J. Am. Chem. Soc.* **2008**, *130*, 5216–5230; h) T. Cusati, G. Granucci, M. Persico, *J. Am. Chem. Soc.* **2011**, *133*, 5109–5123; i) O. Weingart, Z. Lan, A. Koslowski, W. Thiel, *J. Phys. Chem. Lett.* **2011**, *2*, 1506–1509; j) J. Gámez, O. Weingart, A. Koslowski, W. Thiel, *J. Chem. Theory*

Comput. **2012**, *8*, 2352 – 2358; k) J. Gámez, O. Weingart, A. Koslowski, W. Thiel, *Phys. Chem. Chem. Phys.* **2013**, *15*, 11814 – 11821; l) M. Pederzoli, J. Pittner, M. Barbatti, H. Lischka, *J. Phys. Chem. A* **2011**, *115*, 11136 – 11143; m) T. Pancur, F. Renth, F. Temps, B. Harbaum, A. Krüger, R. Herges, C. Näther, *Phys. Chem. Chem. Phys.* **2005**, *7*, 1985 – 1989; n) H. Rau, E. Lueddecke, *J. Am. Chem. Soc.* **1982**, *104*, 1616 – 1620; o) A. Cembran, F. Bernardi, M. Garavelli, L. Gagliardi, G. Orlandi, *J. Am. Chem. Soc.* **2004**, *126*, 3234 – 3243; p) C. Ciminelli, G. Granucci, M. Persico, *J. Chem. Phys.* **2005**, *123*, 174317.

[6] a) D. Rastädter, M. Biswas, I. Burghardt, *J. Phys. Chem. B* **2014**, *118*, 8478 – 8488; b) P. Mondal, M. Biswas, T. Goldau, A. Heckel, I. Burghardt, *J. Phys. Chem. B* **2015**, *119*, 11275 – 11286; c) M. Biswas, I. Burghardt, *Biophys. J.* **2014**, *107*, 932 – 940.

[7] a) R. Turanský, M. Konôpka, N. Doltsinis, I. Štich, D. Marx, *Phys. Chem. Chem. Phys.* **2010**, *12*, 13922 – 13932; b) R. Turanský, M. Konôpka, N. Doltsinis, I. Štich, D. Marx, *ChemPhysChem* **2010**, *11*, 345 – 348.

[8] C. Pace, J. Scholtz, *Biophys. J.* **1998**, *75*, 422 – 427.

[9] H. Nieber, A. Hellweg, N. Doltsinis, *J. Am. Chem. Soc.* **2010**, *132*, 1778 – 1779.

Received: October 14, 2015
Revised: November 17, 2015
Published online: January 6, 2016

